Sensors and Materials, Vol. 28, No. 10 (2016) 1105–1116
MYU Tokyo

S & M 1272

Optical Monitoring Techniques for Navigation during Stereotactic Neurosurgery

Karin Wårdell*

Department of Biomedical Engineering, Linköping University, 581 85 Linköping, Sweden

(Received December 31, 2015; accepted July 1, 2016)

Keywords: deep brain stimulation (DBS), neuronavigation, laser Doppler flowmetry (LDF), diffuse reflectance spectroscopy, radiofrequency (RF) lesioning

Optical techniques are becoming increasingly important in healthcare, as both therapeutic and diagnostic tools. In neurosurgery, photonic technologies such as the microscope have already found widespread use. The overall aim of this paper is to give an overview of optical monitoring methods and their implementation and use in stereotactic and functional neurosurgery. The development steps presented in this paper range from radiofrequency-lesion size estimation using optics to a system adapted for neurosurgical intraoperative navigation during stereotactic deep brain stimulation (DBS) lead implantations. The two main optical methods implemented as intraoperative guidance tools are laser Doppler flowmetry and diffuse reflectance spectroscopy. By combining these fundamental methods with probe designs adapted to stereotactic systems, vessels can be tracked and "bar-codes" of tissue type along pre-defined trajectories used for DBS implantations identified. Examples of the optical methods used in relation to stereotactic DBS implantations are given.

1. Introduction

2015 was dedicated by the United Nations Educational, Scientific and Cultural Organization (UNESCO) as the "International Year of Light and Light-based Technologies".[1] As a global initiative, it highlights the importance of optical technologies in society. In healthcare for example, optical techniques are becoming increasingly essential as both therapeutic and diagnostic tools. In neurosurgery, photonic technologies, such as the conventional white light microscope introduced in the 1950s, have become key features for microsurgery and are used on a daily basis.[2] In recent years, neurosurgical microscopes have also become available with video recording and filters for specific wavelengths that enable the use of dyes. Among these, the blue-light microscope is suitable for the enhancement of malignant brain tumour tissue by means of 5-aminolevulinic acid (5-ALA)-induced fluorescence[3] and the near-infrared (NIR) module for visualizing the vessels with indocyanine green. The blue-light microscope supports the surgeon in the difficult task of defining the border between healthy and tumorous brain tissue. The same fundamental principle can be used to quantify the fluorescence in the tumour or along the tumour border with the help of a hand-held fiber optical probe.[4] Fluorescence techniques can also be used together[5,6] to give both an overview of the field of interest with the microscope, and present the specific well-defined spectral

*Corresponding author: e-mail: karin.wardell@liu.se

ISSN 0914-4935

signature at the border or even inside the tumour by combining the probe with, for example, ultrasound navigation.[7]

The microscope example is one of the few photonic solutions implemented for intraoperative measurements during brain surgery that has found wide clinical use. Neuro-endoscopes are increasingly becoming additional tools for minimally invasive surgery in operating rooms (OR).[8] Other examples of optical techniques with great potential are laser Doppler flowmetry (LDF)[9–12] and laser Doppler perfusion imaging,[13,14] laser speckle contrast imaging,[15] NIR spectroscopy,[16] and optical coherence tomography (OCT).[17]

Another area where optical techniques have been introduced as intraoperative guidance tools is during stereotactic and functional neurosurgery. In functional neurosurgery, a small area of the brain is altered either by radiofrequency (RF) lesioning, i.e., thermal coagulation,[18,19] deep brain stimulation (DBS),[20,21] or cell-line implantation.[22,23] Of these named methods, DBS is the method most commonly used today, with more than 120000 lead implantations worldwide. Its main task is to stimulate a small brain tissue area to give relief in movement-induced disorders such as Parkinson's disease, essential tremor or dystonia. The use of DBS is also being explored in a wide range of neurodisorders including relief from severe psychiatric illness[21] and pain, such as cluster headaches.[24] During stereotactic and functional neurosurgery, the target region is often positioned in the deep brain and therefore not able to be reached with open surgery. Therefore, a navigation system for precise and safe intervention towards the specific brain target is required.[25] Despite the availability of modern surgical planning systems integrating stereotactic fiducials and high-quality magnetic resonance imaging (MRI), it is difficult to foresee a brain shift that can appear due to skull trepanation. Such a shift can result in "a change of the map" and thus increase the necessity for intraoperative monitoring to define the final target in a safe and reliable way. Microelectrode recording (MER)[26] is the most common intraoperative method used during DBS-implantation to record neuronal activity, but it can increase the bleeding incidents.[27] Intraoperative impedance measurement[28] is another well-known method but its resolution is low, especially compared with what can be achieved with optical techniques.[29] During stereotactic neurosurgery, impedance measurements are often performed in relation to RF lesioning, i.e., coagulation of a small brain region in the pallidum or thalamus to alleviate movement disorders.[19] The principle is similar to DBS, i.e., that the cluster of nerves creating the symptoms are affected. However, due to the irreversible effect of the RF technology, many clinical centers prefer to use DBS instead.

Even though the technical developments within biomedical optics for neurosurgery have increased during recent years, most of the optical techniques are still experimental or in the animal exploration stage[30] and have thus not yet been adapted and implemented for clinical neurosurgical settings. The overall aim of this paper is to give an overview of optical sensors and their implementation and use in stereotactic and functional neurosurgery developed at the Department of Biomedical Engineering, Linköping University. First, an RF-lesioning probe with an optical measurement feature is presented. Second, a laser Doppler method for vessel tracking during DBS implantation is reviewed. Third, spectroscopic measurement for "bar-code" identification of tissue type along a pre-defined trajectory is illustrated, and finally, the extraction of chromophores from captured brain spectra is presented. The timeline of the development steps presented in this paper is shown in Fig. 1, i.e., from an RF-lesioning electrode testing device to a system adapted for neurosurgical intraoperative navigation during stereotactic DBS implantation.

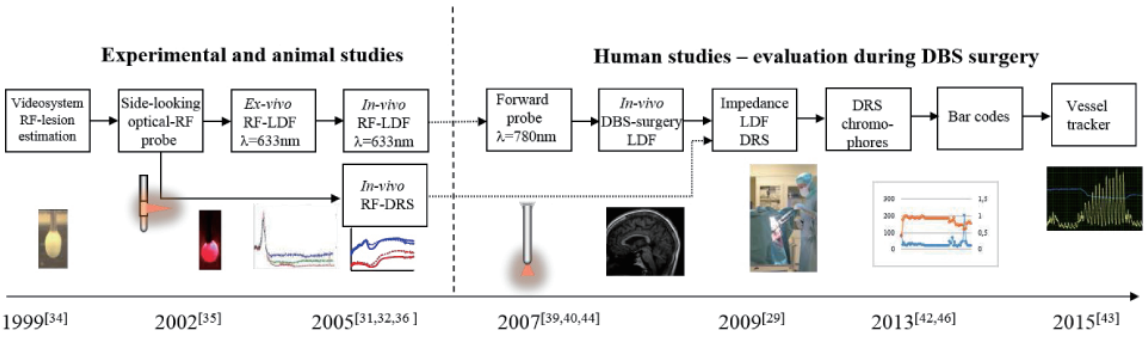

Fig. 1. (Color online) Overview of the development steps of the authors' group, including the RF-electrode tester (far left) towards an intraoperative navigation tool. The years refer to the publication year. RF = radio frequency, LDF = laser Doppler flowmetry, DRS = diffuse reflectance spectroscopy, DBS = deep brain stimulation, STN = subthalamic nucleus, Vim = ventral intermediate nucleus of the thalamus.

2. Combined Optical and RF Probe System

With the aim of intraoperatively determining the RF-coagulation size online, a combination probe for RF lesioning and optical measurements during stereotactic neurosurgery was designed, as shown in Figs. 2(a) and 2(b).[31,32] Its outer dimensions were constructed to fit the Leksell® Stereotactic System (LSS, Elekta Instrument AB, Sweden), i.e., 190 mm long and 2.2 mm wide, with a monopolar tip length of 4 mm. A transparent window above the tip acted as both an insulator and transmitter of the light perpendicular to the measurement object, *e.g.,* the tissue. Optical step index glass fibers [ϕ = 230 µm, numerical aperture (NA) = 0.22] were inserted towards the transparent window, along the rigid stainless steel shaft. A mirror inside the optical window redirected the laser light (λ = 633 nm, P = 2 mW) and backscattered light from the measurement object in four different quadrants by the use of a beam controller. Recorded signals were digitally processed to a perfusion value by using the laser Doppler principle.[9,33] Using LDF, the perfusion (microvascular blood flow) is defined as the average velocity times the concentration of the moving particles (red blood cells) in the measurement volume, and the total backscattered light intensity (TLI), i.e., the DC-signal, displays a greyscale shift during, for instance, an RF lesioning. For a detailed presentation of the signal processing in digital or analogue mode please see Nilsson *et al.*[9] and Karlsson *et al.*[33]

To determine the size of *ex vivo* lesions, various monopolar and bipolar RF-electrode designs (Elekta Instrument AB, Sweden) were first evaluated experimentally using both egg white and an albumin solution, together with a video recording system and the Leksell® Neuro Generator (LNG, Elekta Instrument AB, Sweden).[34] Systematic variations of the coagulation temperature made it possible to determine the size, shape and time course of the clots as created in the albumin or egg white with the RF electrodes. By adding microspheres to the albumin solution, laser Doppler signals were recorded simultaneously to the coagulation, and the changes of the perfusion and TLI signals were matched to the clot generation and size, respectively, as shown in Figs. 2(c) and 2(d). Secondly, the lesion size was estimated *in vivo* using a stereotactic porcine brain model by utilizing MRI and histology analysis. These *in vivo* lesions were compared with preoperative electrode coagulations in albumin.[35] Thirdly, the combined optical and RF-electrode system presented above, shown in Figs.

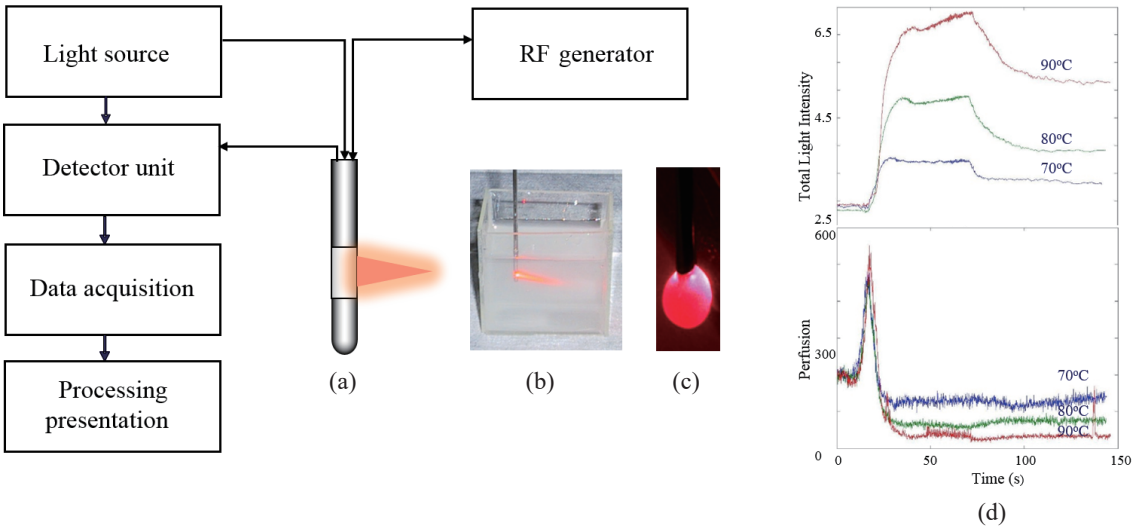

Fig. 2. (Color online) (a) Optical RF probe system. An optical window acts as an insulator and transmits the light to and from the tissue via a mirror. (b) Photograph of the probe and light beam. (c) Coagulation in albumin using the RF electrode with optical fibers and He-Ne laser light. (d) Laser Doppler measurements of perfusion and TLI during RF coagulation in albumin with scatters at 70, 80, and 90 °C.

2(a) and 2(b), was used during *in vivo* lesioning in the porcine brain.[32] It was thus confirmed that the optical recordings could be used as an *in vivo* online indicator of the lesioning by studying the change in TLI and microcirculation (perfusion) reduction in relation to the increased lesion size. An example of recorded LDF signals is given in Figs. 3(a) and 3(b) for simultaneous TLI and perfusion recordings during the entire *in vivo* RF lesioning. It is clearly seen that both signals are decreased in parallel to the growth of the lesion. Diffuse reflectance spectra (DRS) investigations performed during the same study revealed that by using a laser in the NIR region, *e.g.,* 780 nm instead of 633 nm, a better distinction between grey and white matter as well as between lesioned and unlesioned tissue could be found.[36] In Fig. 3(c), examples of spectra recorded in grey and white porcine matter before and after RF lesioning are presented with the 633 and 780 nm wavelengths marked. It is clearly seen that lesioned grey matter is brighter than unlesioned matter and that the largest distinction between tissue types is found around 700–800 nm. This finding is consistent with investigations of light interaction with tissue performed by Giller and colleagues,[37,38] who also showed that NIR light is more suitable for brain tissue-type discrimination. Furthermore, both groups have suggested using angular probes for emitting the light perpendicular from the probe shaft.[32,38] Unfortunately, angular probes are more difficult to construct than forward-looking probes, and may also require a more advanced data collection system if measurements need to be performed in several quadrants during the same measurement session.

Over the last decade, the number of RF-lesioning procedures for movement disorders has been reduced significantly, and they are more often replaced by DBS implants. As the stereotactic part of the surgical procedure is very similar for the two methods, the challenge in reaching the preplanned target in a safe and reliable way remains. For DBS implantations, however, a pure intraoperative guidance tool is sufficient, as no direct measurements can be made with optics of the tissue volume influenced from the electrical stimulation. For such investigations, patient-specific finite element method modelling and simulations of the electric field extension can be performed postoperatively.[39,40]

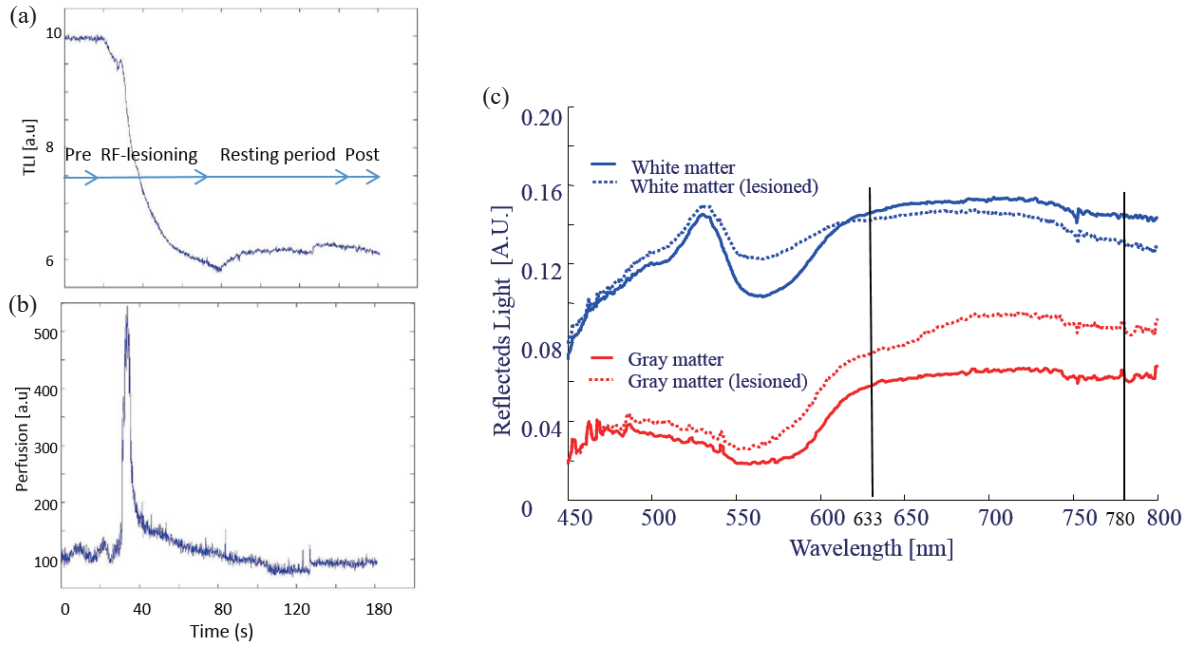

Fig. 3. (Color online) (a) TLI and (b) microcirculation (perfusion) changes during *in vivo* RF lesioning using the combined RF and optical probe (λ = 633 nm, 2 mW, T = 80 °C). (c) Reflectance spectra recorded in white and grey matter before and after RF lesioning. The most common laser Doppler wavelengths, λ = 633 nm and λ = 780 nm, are marked.

3. LDF as Navigational Tool during Stereotactic Neurosurgery

A more simplified design, compared to the angular probe, is to use a forward-looking probe, as shown in Fig. 4(a), with a smoothly rounded and carefully polished tip for minimizing tissue trauma. Such a probe can have a dual guiding function and act as both a "vessel alarm" and a tissue-type identifier. The forward-looking probe[41] was constructed with the same outer dimensions as a standard RF-electrode. However, the diameter of the probe was reduced to 1.5 mm in the last 30 mm towards the tip. This size complies well with the outer diameter of DBS electrodes, which is around 1.3 mm. Four optical fibers were aligned along the interior side of the probe shaft all the way towards the tip, thus making it possible to investigate the tissue in the vicinity of the tip. The laser light was changed from 633 to 780 nm, a wavelength used in commercially available LDF systems, *e.g.*, the Periflux (Perimed AB, Sweden). The output power was still kept below 1 mW to stay within the range of a Class II-device. By using the Periflux, the perfusion and DC (TLI) signals could be directly sampled from the device without any separate digital signal processing of the raw Doppler spectra. In-house software developed in LabVIEW (National Instruments, Inc., TX, USA) was designed for data collection and presentation, and the laser Doppler system was adapted for recording both the microcirculation (perfusion) and TLI now displaying the brain tissue in shades of grey.[42] Figure 4(b) presents the laser Doppler principle and Fig. 4(c) the setup of the system with the forward-looking probe positioned in the LSS. Using this design and construction, the optical probe and cable were able to be sterilized in accordance with the

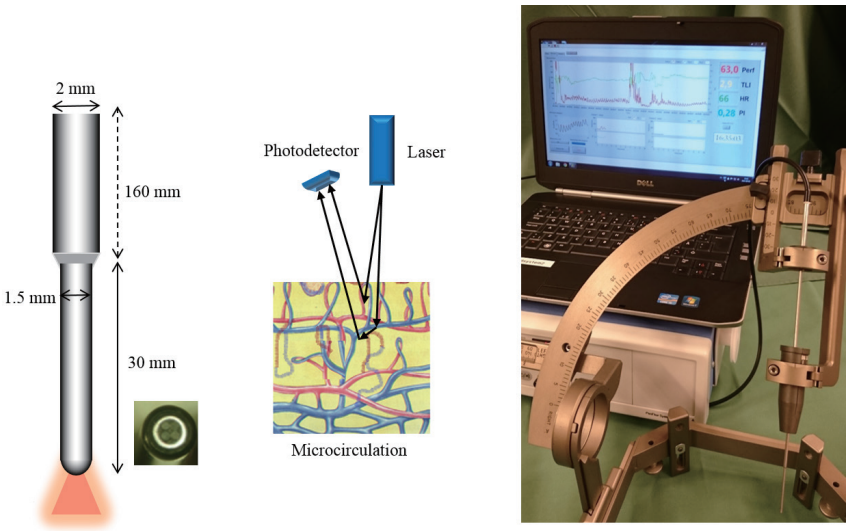

Fig. 4. (Color online) (a) Principle of forward looking measurement probe with cross-sectional photograph of the tip presenting the four optical fibers. (b) The laser Doppler principle: backscattered moving red blood cells in the microvascular network give rise to a Doppler shift processed to the perfusion signal after photodetection. (c) The probe positioned in the Leksell® Stereotactic System with recorded signals presented on the screen.

STERRAD® protocol.[43] An optical cable of at least 4 m is recommended to keep the measurement equipment at a safe distance from the operation area, and thus optically isolated from the surgical field.

The system has so far been used in more than 100 DBS lead implantations (approved by the local ethics committee, M182-04, T54-09) in brain target areas commonly used to give relief in movement disorders such as Parkinson's disease, essential tremor and dystonia.[41,44] Examples of such deep brain targets are the subthalamic nucleus (STN) [Fig. 5(a)], the ventral intermediate nucleus (Vim) of the thalamus, the globus pallidus internus (GPi) and the Zona incerta (Zi).[25] These targets are small, for example, the STN is disc shaped and approximately $8 \times 6 \times 5$ mm^3.[45]

During a stereotactic implantation of DBS electrodes, the optical probe can be used as a guide for creating the trajectory towards the preplanned target prior to the implantation of the DBS lead [Fig. 5(b)]. At the same time as the probe is inserted, the microcirculation and tissue greyness can be recorded in front of the tip, i.e., before the tissue is even touched. With the use of an in-house hand driven mechanical device[44] designed to fit the LSS, the surgeon can control the insertion of the probe in sub-millimeter steps all the way from the cortex to the respective deep brain structures [Fig. 5(c)]. In between each movement, the probe must be kept still for 5–10 s during the actual sampling of the signals at each site. This waiting time is essential for the laser Doppler recording, as the perfusion signal is extremely sensitive to external movements caused by introducing the probe, i.e., no reliable measurement can be obtained during a movement. An example of a laser Doppler recording with the LSS and the mechanical device in the deep part of the brain towards the STN is presented in Fig. 5(d), and a view from the OR is seen in Fig. 5(e). A high-perfusion spot is shown at 3 mm from the STN in Fig. 5(d). The peaks, marked with red bars, between the stable perfusion signals present the movements of the mechanical device from one site to the next during

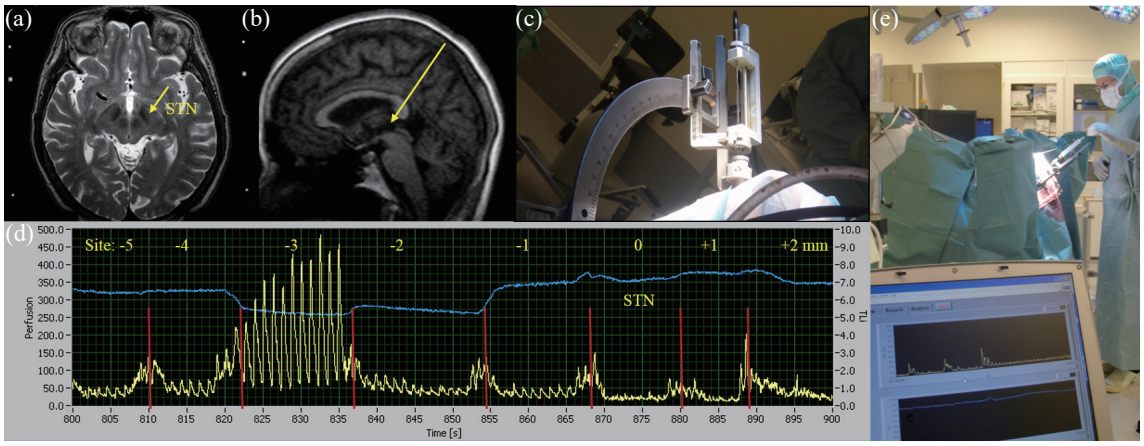

Fig. 5. (Color online) (a) Axial MRI with marked fiducials and the STN. (b) Sagittal MRI illustrating a typical trajectory towards the target (yellow arrow). (c) Measurement probe positioned in the Leksell® Stereotactic System and mechanical device for step-wise insertion along the trajectory during deep brain stimulation surgery. (d) Example of *in vivo* measurement towards the STN. The yellow curve represents the microcirculation (perfusion) signal and the blue the TLI. The red marks in the yellow curve show the movement of the mechanical device, which are used as position markers for the creation of a TLI curve in Fig. 6. (e) View from the operating room.

clinical recording. Within a few seconds from the movement, the laser Doppler signal is stable and the captured signals allow calculation of, for instance, mean perfusion, heart rate and peak-to-peak of the microcirculation as well as the TLI at a specific position in the brain tissue. The microcirculation signal can also be used to track larger vessels along the trajectory,[46] and the TLI signals have been used to determine "bar-codes" towards two of the most common DBS targets; the STN and the Vim.[44] Figure 6 shows perfusion and TLI signals post-processed to "bar-codes" following insertion with the mechanical device at 1 mm steps towards the STN. In this specific case, the patient already had an RF lesion, which was passed during the probe insertion. This is seen as an unchanged flat line in both the perfusion and TLI signals. The perfusion was low, except for 3 mm from the STN target, where a high-perfusion spot was found, similarly to the peak also seen in Fig. 5(d). This site most likely relates to a small vessel structure in the vicinity of the probe tip. One millimeter away, the perfusion becomes low again.

4. DRS as a Navigational Tool during Stereotactic Neurosurgery

In a similar way to the TLI signal from the laser Doppler system, DRS can be used to display the shades of grey matter as well as white matter of the brain in a relative manner. This, however, requires that the spectra are processed in the NIR region. One of the optical fibers from the probe is then connected to a white lamp (AvaLight-Hal-S, Avantes, The Netherlands) and the receiving fiber attached to the spectrometer (AvaSpec-2048-2, Avantes, The Netherlands). The data collection and presentation is also controlled by a LabVIEW interface. Giller *et al.*[37] used this principle to create curves of light intensity changes along insertion trajectories during DBS implantations. This research group used slope algorithms for grey-white matter classification, a method that applies

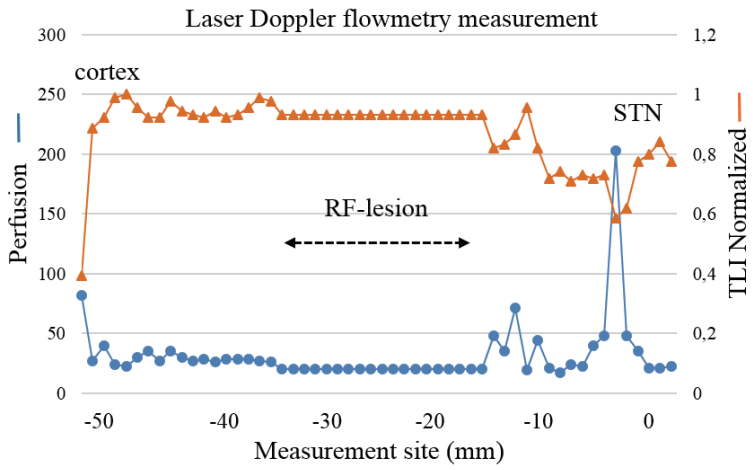

Fig. 6. (Color online) LDF measurement in 1 mm steps using the forward looking probe. Recordings were performed from the cortex towards the STN. The probe passes a previous RF lesion. A high perfusion spot is seen 3 mm from the STN (blue curve). The data was extracted from the total light intensity recorded with LDF.

the fitting of a straight line to the collected unprocessed reflectance spectra in an NIR-interval. The Linköping concept instead uses a very narrow wavelength interval of around 780 nm for the creation of curves by cutting out the intensity from each separate spectrum, as shown in Fig. 7(a). A very high correlation was found between the two methods of analysis[47] and also with the LDF-TLI approach, which uses a 780 nm laser.[41] The single wavelength approach using DRS was implemented as an on line feature in the LabVIEW software.[29] This made it possible to record grey-white tissue boundary changes during DBS implantation without interference from external movements, but without the microcirculation information feature. An example is presented in Fig. 7(b) where a continuous recording of spectra with DRS was performed from the cortex towards the GPi. At this time point, no mechanical device was used and thus the relation to the anatomical positions can only be estimated and so is not an exact anatomical match.

An additional approach for increasing knowledge about brain tissue is to extract chromophore information from the recorded *in vivo* reflectance spectra. Johansson developed an algorithm for quantifying chromophore content from spectra recorded in brain tissue.[48] The method was applied on spectra captured in grey and white matter as well as targets common for DBS implantations. Chromophores such as various types of hemoglobin, lipofuscin, melanin, and different cytochromes were estimated for the brain structures studied. An example recorded in the cortex is presented in Fig. 7(c).[49] With the help of the oxygenated hemoglobin (HbO_2) and deoxygenated hemoglobin (Hb) spectra from brain tissue, an estimation of the oxygen saturation (SO_2) can be achieved by curve fitting to known absorption spectra. The present work in the Linköping group focuses on improving the oxygen saturation algorithm for *in vivo* on line recording in brain tissue[50] in relation to, for example, traumatic brain injury in the neuro-intensive care unit, and thus also adaptation and implementation of the methods for monitoring of both microcirculation[12] and tissue oxygenation during brain surgery.

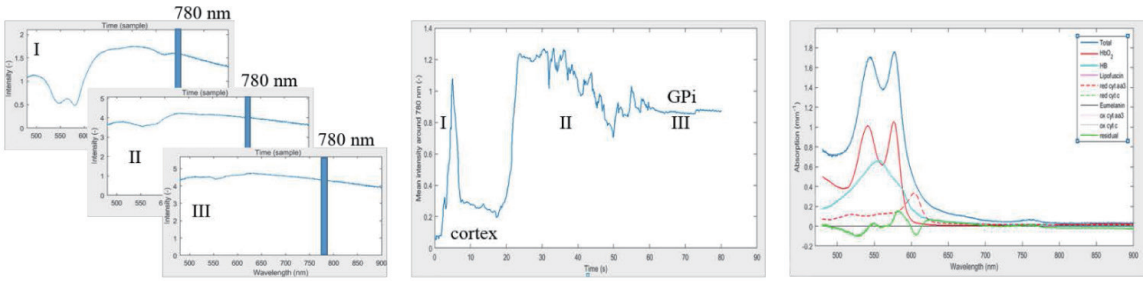

Fig. 7. (Color online) (a) Reflectance spectra with 780 nm marked to symbolize how the time curve is built up. (b) Time curve built from cortex to GPi during continuous insertion of the forward looking probe. (c) Absorption spectra extracted for various chromophores and from the first spectrum presented in (a).

5. Measurement Depth and Resolution

Light interaction with tissue is affected by several aspects including wavelength, probe design, and the tissue's scattering and absorption characteristics. Investigations using Monte Carlo simulations show that the optical sampling depth, sometimes also denoted as the "look ahead distance" (LAD) in brain tissue is around 1 mm.[51–54] In the NIR region and for small fiber separation, Monte Carlo simulations show that grey matter has a slightly increased LAD compared with white matter. Johansson[48] studied the LAD for different layer combinations and found from simulations that grey matter compared to white matter showed LAD to be about two times longer compared to white over grey layers due to the lower scattering. Both white and grey matter overlaid with non-scattering cerebrospinal fluid increased the LAD by several millimeters and for a layer of blood it decreased below fractions of a millimeter due to the high absorption. Nevertheless, the optical resolution is significantly higher than the MRI resolution commonly used when planning a functional neurosurgical procedure. For this, an MRI with a stereotactic frame on the patients head is usually performed with 2 mm trans axial slices and has also been used for planning DBS implantations during our studies when the optical measurements were performed [Figs. 5(a) and 5(b)]. A recent study on patients implanted with DBS electrodes using optical guidance has shown that both TLI, i.e., grey-white tissue differences, and microvascular changes can be recorded with 0.5 mm resolution, and thus local blood flow and TLI peaks can be identified with this resolution.[46] An optical resolution of about 0.5–1 mm can therefore be considered reasonable in stereotactic and functional neurosurgery, especially as the DBS leads and RF electrodes are about 1.3 mm and 1.5–2 mm in diameter, respectively. These diameters are, on the other hand, rather large compared to the nuclei, which measure a few millimeters up to about 1 cm.

6. Conclusions and Future Directions

In this paper, optical methods for intraoperative guidance during stereotactic and functional neurosurgery have been demonstrated. By combining different optical approaches, more information about cerebral blood flow parameters and tissue types can be gained and thus used to

increase both safety and precision during stereotactic neurosurgery. An example already presented is the combination probe for RF lesioning and optical verification of the coagulation, another is to make use of both LDF and DRS in the same measurement session to gain information from both about tissue type, i.e., grey-white boundaries, chromophore content, SO_2 and the tissue's microcirculation. As the optical fibers are thin (125 to 250 μm in diameter), all these features are possible to incorporate in one probe design, which can be used during neurosurgery, for example, as an on line tool in the OR, during stereotactic and functional neurosurgery, and possibly also in the neuro-intensive care unit for monitoring cerebral microvascular blood flow. Other options could be to combine LDF and DRS with fluorescence spectroscopy for diagnostic purposes during both open tumour surgery and stereotactic biopsies. We are presently working on a concept combining the "vessel alarm" function and the 5-ALA induced fluorescence detection of malignancy in a real-time optical biopsy concept. An additional future adaptation could be to incorporate the present probes with OCT. Successful attempts have been made in studying brain tissue *in vivo* by several groups.[17,55,56] So far, however, these protocols are applicable for animals only. In the same way that RF lesioning can be combined with optics, it may be possible that intraoperative MER and local field potential measurements, commonly used during DBS implantation, could be used together as a multiparametric tool. Giller and colleagues[38] have previously presented an example of the combined use of NIR pectroscopy and MER. To completely close the loop in the use of photonics, the navigational tools should be combined with optical therapeutic tools, *e.g.,* optogenetic[57,58] or optothermal neuronal stimulation[59] for individual nerve cell interaction with light and thus precise tailoring of the stimulated tissue volume. Despite years of intensive research and many fundamental discoveries and deeper insights of nervous system function based on animal studies,[60] the optogenetic technique has not yet been adopted for human use, and DBS will remain the gold standard for brain stimulation in the clinical setting in the near future.

In conclusion, optical techniques have already proven useful as support systems in stereotactic brain surgery, for example, as direct navigational tools for "vessel tracking" and "bar-code" identification of tissue during DBS implantation. Further evaluation of the optical techniques' clinical performance is, however, necessary, together with tailoring of the probes and measurement methods to the respective clinical indications. Furthermore, an improved methodology for translating optical techniques used for animal studies into clinical use will be required to make this transition in a safe, efficient, cost-effective and user-friendly manner.

Acknowledgements

I am deeply grateful for all present and previous group members who have contributed to the different steps of the technical and experimental developments as well as the translation of the methods for clinical use. I am also very grateful to all the clinical colleagues who have made the intraoperative measurements possible. Please see the reference list for names.

These studies were supported by Group Grant No. 311-2006-7661 received from the Swedish Research Council (VR), the Swedish Governmental Agency for Innovation Systems (Vinnova) and the Swedish Foundation for Strategic Research (SSF). The Parkinson Foundation at Linköping University, and the VR-Project Grants Nos. 621-2010-4216 and 621-2013-6078 supported different parts of the presented projects.

References

1 Lightsources: International Year of Light and Light-Based Technolgies, http://www.light2015.org (accessed 24 November 2015).
2 K. Uluc, G. C. Kujoth, and M. K. Baskaya: Neurosurg. Focus **27** (2009) E4.
3 W. Stummer, U. Pichlmeier, T. Meinel, O. D. Wiestler, F. Zanella, and H. J. Reulen: Lancet Oncol. **7** (2006) 392.
4 N. Haj-Hosseini, J. Richter, S. Andersson-Engels, and K. Wårdell: Lasers Surg. Med. **42** (2010) 9.
5 W. Stummer, J. C. Tonn, C. Goetz, W. Ullrich, H. Stepp, A. Bink, T. Pietsch, and U. Pichlmeier: Neurosurgery **74** (2014) 310.
6 N. Haj-Hosseini, J. Richter, and K. Wårdell: Photodiagnostics in Brain Tumor Surgery, 16th Nordic-Baltic Conference on Biomedical Engineering & Medical Physics Oct. 14–16, 2014.
7 J. C. Richter, N. Haj-Hosseini, S. Andersson-Engel, and K. Wårdell: Lasers Surg. Med. **43** (2011) 8.
8 G. Zada, C. Liu, and M. L. Apuzzo: World Neurosurg. **79** (2013) S3.
9 G. E. Nilsson, T. Tenland, and P. A. Öberg: IEEE Trans. Biomed. Eng. **27** (1980) 597.
10 R. L. Haberl, A. Villringer, and U. Dirnagl: Acta Neurochirurgica. Supplementum **59** (1993) 64.
11 J. P. Dreier, S. Major, A. Manning, J. Woitzik, C. Drenckhahn, J. Steinbrink, C. Tolias, A. I. Oliveira-Ferreira, M. Fabricius, J. A. Hartings, P. Vajkoczy, M. Lauritzen, U. Dirnagl, G. Bohner, and A. J. Strong: Brain **132** (2009) 1866.
12 P. Rejmstad, G. Åkesson, O. Åneman, and K. Wårdell: Med. Biol. Eng. Comput. **54** (2016) 123.
13 K. Wårdell, A. Jakobsson, and G. E. Nilsson: IEEE Trans. Biomed. Eng. **40** (1993) 309.
14 A. Raabe, D. Van De Ville, M. Leutenegger, A. Szelenyi, E. Hattingen, R. Gerlach, V. Seifert, C. Hauger, A. Lopez, R. Leitgeb, M. Unser, E. J. Martin-Williams, and T. Lasser: Neuroimage **44** (2009) 1284.
15 A. B. Parthasarathy, E. L. Weber, L. M. Richards, D. J. Fox, and A. K. Dunn: J Biomed. Opt. **15** (2010) 066030.
16 D. J. Davies, Z. Su, M. T. Clancy, S. J. Lucas, H. Dehghani, A. Logan, and A. Belli: J. Neurotrauma **32** (2015) 933.
17 S. W. Jeon, M. A. Shure, K. B. Baker, D. Huang, A. M. Rollins, A. Chahlavi, and A. R. Rezai: J. Neurosci. Methods **154** (2006) 96.
18 L. V. Laitinen: Stereotact. Funct. Neurosurg. **74** (2000) 1.
19 H. Hirabayashi, M. I. Hariz, K. Wårdell, and P. Blomstedt: Stereotact. Funct. Neurosurg. **90** (2012) 307.
20 A. L. Benabid: Current Opinion Neurobiol. **13** (2003) 696.
21 M. Hariz, P. Blomstedt, and L. Zrinzo: Mov. Disord. **28** (2013) 1784.
22 P. Brundin, R. A. Barker, and M. Parmar: Prog. Brain Res. **184** (2010) 265.
23 R. A. Barker, J. Drouin-Ouellet, and M. Parmar: Nat. Rev. Neurol. **11** (2015) 492.
24 S. G. Boccard, E. A. Pereira, and T. Z. Aziz: J. Clin. Neurosci. **22** (2015) 1537.
25 S. Hemm and K. Wårdell: Med. Biol. Eng. Comput. **48** (2010) 611.
26 R. E. Gross, P. Krack, M. C. Rodriguez-Oroz, A. R. Rezai, and A. L. Benabid: Mov. Disord. **21** (2006) S259.
27 L. Zrinzo, T. Foltynie, P. Limousin, and M. I. Hariz: J. Neurosurg. **116** (2012) 84.
28 L. Zrinzo and M. Hariz: Textbook of Stereotactic and Functional Neurosurgery (Springer, Heidelberg, 2008).
29 J. D. Johansson, P. Blomstedt, N. Haj-Hosseini, A. T. Bergenheim, O. Eriksson, and K. Wårdell: Stereotact. Funct. Neurosurg. **87** (2009) 105.
30 E. M. Hillman: J. Biomed. Opt. **12** (2007) 051402.
31 J. Antonsson, O. Eriksson, and K. Wårdell: J. Biomed. Opt. **10** (2005) 034020.
32 J. Antonsson, O. Eriksson, P. Lundberg, and K. Wårdell: Stereotact. Funct. Neurosurg. **84** (2006) 118.
33 M. G. Karlsson, H. Casimir-Ahn, U. Lönn, and K. Wårdell: Med. Biol. Eng. Comput. **41** (2003) 255.
34 O. Eriksson, K. Wårdell, N. E. Bylund, G. Kullberg, and S. Rehncrona: Neurol. Res. **21** (1999) 89.
35 O. Eriksson, E. O. Backlund, P. Lundberg, H. Lindstam, S. Lindström, and K. Wårdell: Neurosurgery **51** (2002) 781.
36 J. Antonsson, O. Eriksson, and K. Wårdell: Adv. Biomed. Clin. Diagn. Syst. **4958** (2003) 242.
37 C. A. Giller, H. L. Liu, P. Gurnani, S. Victor, U. Yasdani, and D. C. German: J. Neurosurg. **98** (2003) 1299.
38 C. A. Giller, H. Liu, D. C. German, D. Kashyap, and R. B. Dewey: J. Neurosurg. **110** (2009) 263.
39 C. R. Butson, S. E. Cooper, J. M. Henderson, B. Wolgamuth, and C. C. McIntyre: Neuroimage **54** (2011) 2096.

40 K. Wårdell, Z. Kefalopoulou, E. Diczfalusy, M. Andersson, M. Åström, P. Limousin, L. Zrinzo, and M. Hariz: Neuromodulation **18** (2015) 90.
41 K. Wårdell, P. Blomstedt, J. Richter, J. Antonsson, O. Eriksson, P. Zsigmond, A. T. Bergenheim, and M. I. Hariz: Stereotact. Funct. Neurosurg. **85** (2007) 279.
42 K. Wårdell, C. Fors, J. Antonsson, and O. Eriksson: Conf. Proc. IEEE Eng. Med. Biol. Soc. **2007** (2007) 4083.
43 P. T. Jacobs: Johnson & Johnson, White Paper International Version Report (1999).
44 K. Wårdell, P. Zsigmond, J. Richter, and S. Hemm: Neurosurgery **72** (2013) 127.
45 C. D. Hardman, J. M. Henderson, D. I. Finkelstein, M. K. Horne, G. Paxinos, and G. M. Halliday: J. Comp. Neurol. **445** (2002) 238.
46 K. Wårdell, S. Hemm-Ode, P. Rejmstad, and P. Zsigmond: Stereotact. Funct. Neurosurg. **94** (2016) 1.
47 J. Antonsson, O. Eriksson, P. Blomstedt, A. T. Bergenheim, I. H. M, J. Richter, P. Zsigmond, and K. Wårdell: J. Neural Eng. **5** (2008) 185.
48 J. D. Johansson: J. Biomed. Opt. **15** (2010) 057005.
49 J. D. Johansson and K. Wårdell: J. Biophotonics **6** (2013) 435.
50 P. Rejmstad, D. J. Johansson, N. Haj-Hosseini, and K. Wårdell: J. Biophotonics **20** (2016).
51 J. D. Johansson, I. Fredriksson, K. Wårdell, and O. Eriksson: J. Biomed. Opt. **14** (2009) 044040.
52 Z. Qian, S. Sunder, G. Yeqing, C. Giller, and H. Liu: Opt. Express **11** (2003) 1844.
53 M. Larsson, W. Steenbergen, and T. Strömberg: J. Biomed. Opt. **7** (2002) 236.
54 A. Jakobsson and G. E. Nilsson: Med. Biol. Eng. Comput. **31** (1993) 301.
55 C. P. Liang, J. Wierwille, T. Moreira, G. Schwartzbauer, M. S. Jafri, C. M. Tang, and Y. Chen: Opt. Express **19** (2011) 26283.
56 Y. Xie, N. Martini, C. Hassler, R. D. Kirch, T. Stieglitz, A. Seifert, and U. G. Hofmann: Frontiers Neuroeng. **7** (2014) 34.
57 V. Gradinaru, M. Mogri, K. R. Thompson, J. M. Henderson, and K. Deisseroth: Science **324** (2009) 354.
58 I. Ozden, J. Wang, Y. Lu, T. May, J. Lee, W. Goo, D. J. O'Shea, P. Kalanithi, I. Diester, M. Diagne, K. Deisseroth, K. V. Shenoy, and A. V. Nurmikko: J. Neurosci. Methods **219** (2013) 142.
59 R. Liljemalm, T. Nyberg, and H. von Holst: Lasers Surg. Med. **45** (2013) 469.
60 K. Deisseroth: Nature Neurosci. **18** (2015) 1213.